Thermal Conductivity of the ZrO_2 Based Composite Coatings Prepared by Gas Tunnel Type Atmospheric Plasma Spraying †

ZHANG Jialiang* and KOBAYASHI Akira **

Abstract

ZrO_2 based thermal barrier coatings prepared using plasma spraying are frequently modified by mixing some kinds of additives such Al_2O_3, in order to improve their oxygen ion resistance. Using gas tunnel type plasma spraying, characterized by higher plasma temperature and better stability than traditional arc plasma spraying, zirconia based composite coatings with various mixing ratios of alumina were used to generate graded-functional microstructures. Because of the plasma stability, the coating micro-structural parameters such as the thickness, mixing ratio of alumina and porosity were well reproduced by keeping the spraying parameter constant. A group of coating samples was prepared in this research to be almost the same thickness but different composition ratios. The surface and cross-sectional morphologies of the coatings were examined by SEM (Scanning Electron Microscope) and OM (Optical Microscopy). The coating thickness was measured and the alumina content ratio was assessed from the SEM photos, while the coating porosity (the porosity profile over the cross-section and the average porosity) was obtained from the image analysis of the optical photos. The coating hardness was measured with a micro Vicker hardness tester and the thermal conductivity was measured based on the principle of steady heat flux between two parallel hot plates. The results showed that the addition of alumina increased the coating hardness and lowered the coating porosity, while not reducing the thermal resistance of the coating layers.

KEY WORDS: (ZrO_2 based thermal barrier coatings), (Coating thermal conductivity), (Parallel hot plates method), (Gas tunnel type plasma spraying)

1. Introduction

Plasma sprayed zirconia based composite coatings are frequently used as thermal barrier coatings to many applications because of their very low thermal conductivity and porous microstructure. Although it has been found that plasma sprayed zirconia coatings exhibit lower thermal conductivity than zirconia coatings prepared by another deposition method suitable for thermal barrier coatings, the Electron Beam Physical Vapor Deposition (EB-PVD), the sprayed coating microstructure puts also observable effect on the thermal conductivity even if the plasma sprayed zirconia coatings show very low thermal conductivity[1]. These kinds of TBC coatings are characterized in microstructure with lamellae and micro pores, which are helpful respectively for the coating thermal resistance vertical to the coating surface and for lowering the residual stress in the coating[2]. However, zirconia is a ceramic with very high melting point and therefore it is difficult to ensure all the sprayed powders heated enough to be fully molten in spraying plasmas. One of the authors suggested a gas tunnel type plasma spraying technique[3], which can produce more stable arc plasma torches with higher temperature. With this kind of spraying plasma, zirconia coatings consisting of lamellae of fully molten splats have been obtained. The zirconia coatings show high hardness and good thermal resistance [4]. However, on the other hand, crystalline zirconia is a solid ion conductor, through which oxygen ions can transport[5]. If the zirconia coatings have a more order constructure, such as a more order stack of lamellae, in fact which is the true case for the gas tunnel type plasma sprayed coatings, the lamellae share bigger interfaces and therefore will offer the transporting oxygen ions a lower resistance. The oxygen ions induce an oxidation reaction at the metal substrate surface and an oxide layer grows gradually to result in the spalling of the coating. The coating spallation is the mean reason for failure of the coating performance[6].

In order to overcome the spallation of zirconia coatings, alloy bonding layers are frequently introduced into the process of coating preparation[7]. The bonding layer is normally an alloy with high oxidation resistance and therefore only few kinds of candidate alloy are found. Thus the application of bonding layers for thermal barrier coating preparation was constrained by two difficulties: one, how to find the suitable alloy for various kinds of substrates and the other, the deposition step of bonding layers makes the procedure more complicated[8]. Searching for any other measures to solve the spallation problem is always simultaneous with the search for bonding layer candidates. Mixing of Al_2O_3 into zirconia coatings is claimed to be an efficient way of retarding the spallation[9]. Zirconia composite coatings with alumina additive have been improved with decreased ion conductivity and lower porosity because the alumina additive distorts the stacking of zirconia lamellae and alumina is lower in melting point than zirconia. However, the addition of alumina modifies the microstructure of the composite coatings and therefore possibly reduces the thermal resistance of the coatings, because the alumina additive with higher thermal conductivity than zirconia is worse for the coating thermal resistance. In this paper, the thermal conductivity of zirconia composite coatings with alumina

† Received on May 12th, 2006
* Foreign Guest Researcher
** Associate Professor

Transactions of JWRI is published by Joining and Welding Research Institute, Osaka University, Ibaraki, Osaka 567-0047, Japan

additive prepared on SUS304 substrates by gas tunnel type plasma spraying was measured and the effect of the alumina additive on the coating thermal conductivity was investigated based on microstructure characterization of the coatings.

Several methods have been setup to measure the thermal conductivity or thermal diffusivity, such as the primary parallel hot plates method, hot plate or hot wire methods, pulsed hot wire method, pulsed heating source methods laser flash, electron beam, ion beam as pulsed heating sources) and ultrasonic harmonics resonance method[10, 11]. However, few of these methods are suitable for coating measurement. In principle, pulsed heating source methods should be more precise for coating measurement application because those methods are based on the thermal diffusivity measurement, but all the pulsed heating source methods need the coating samples separated from substrates and for most cases it is very difficult to peel the coatings from the substrates. In this paper, instead of any pulsed heating methods, the primary parallel hot plates method was used to measure the coating thermal conductivity vertical to the coating surface, while the application of the laser flash heating method to pure stainless steel was used as the calibration procedure for the parallel hot plates method.

2. Experimental Description

2.1 Atmospheric plasma spraying assembly (APS)

Figure 1 shows schematically the gas tunnel type plasma spraying setup. The discharge system has a specially designed spacer between the two anodes, which is characterized by gas channels on its wall in such a pattern that the gas flow injects into the hollow cavity of the spacer and forms a gas tunnel in its axial region. The plasma firstly forming in the hollow anode and then emitting like a flame outside the exit is well confined in the tunnel due to the thermal pinch effect and can be much higher in temperature and more stable than traditional free-standing arc torches[12].

The plasma spraying setup consists of one trigger cathode rod, one hollow anode and one nozzle anode and thus forms a two stage cascade arc scheme. More detail of the system is presented in Ref 13. Facing the plasma, a two-dimension movable substrate holder is equipped to vary the distance between the substrates and the nozzle anode exit. The first-stage of the system is powered by a DC power source which can provide current as high as 100A and power as high as 10KW and triggered by a high voltage as high as 3KV at a pulsation

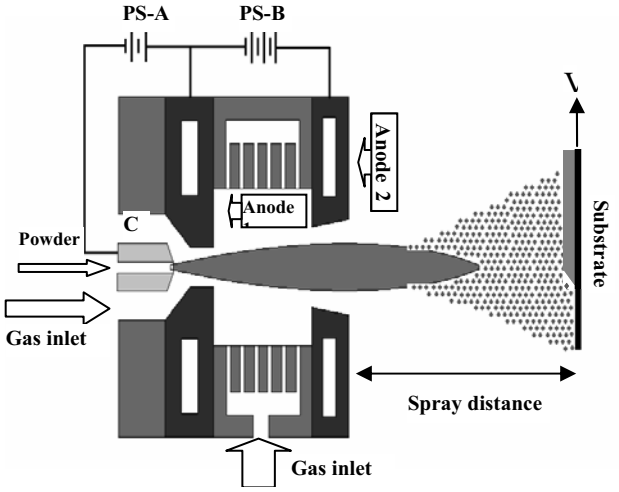

Fig.1 Schematic of the plasma spraying setup.

Table 1 Spraying conditions.

Powder:	ZrO_2:Al_2O_3
Power input,P (kW):	20
Gas flow rate, Q (l/min):	150
Powder feed gas, Q_f(l/min):	10
Spraying distance, L (mm):	40
Deposition time, t (s):	20
Substrate:	SUS 304
Ratio of Al_2O_3:	100%, 50%, 20%, 0
Coating thickness:	215-250μm

frequency of 120Hz, while the second-stage is powered by another more powerful DC supply that can output current as high as 500A and power of 30KW to amplify the plasma power. For the two stages, two gas inlets are used to feed working gas. The working gas for the first stage is fed through the rear inlet around the trigger electrode, while the carrier gas for the second stage is fed from the channels on the spacer wall.

Although the spraying system is always operated in the atmosphere, it is installed in a close chamber to avoid the powder residues from polluting the Lab and to shield the torch from the ambient air.

In the present research, working argon gas is fed into the gap between the first-stage electrode pair at a nominal gas flow rate of 50l/min and also carrier gas of argon is fed into the spacer cavity at a nominal rate of 150l/min. Normally, based on the present configuration, the first-stage is successfully maintained with an arc voltage of 40-55V and current of 60-80A, while the second-stage discharge is successfully maintained with a voltage of 30-40V and current of 300-450A.

The gas tunnel type plasma spraying was used to deposit zirconia coating with different mixing ratio of alumina on SUS 304 substrates under a discharge power of 20kW. The procedure to produce high hardness ceramic coatings by means of the gas tunnel type plasma spraying has been described in the previous papers[14]. Briefly speaking, the sprayed powder is fed into the plasma flame through the rear feeding inlet inside the trigger cathode rode. Coatings are formed on the substrates traversed at a spraying distance L=40mm. Before spraying, the square substrate plates of stainless steel SUS304 were previously sandblasted and cleaned in acetone. The substrate is 50mmX50mmX3mm. In this research, the deposition time for all the samples was 20μs. By feeding powder mixtures with different weight mixing ratios, 100%ZrO_2, 50%ZrO_2-50%Al_2O_3, 80%ZrO_2-20%Al_2O_3, 0% ZrO_2, (mole mixing ratios, 100%ZrO_2, 59%ZrO_2-41%Al_2O_3, 85%ZrO_2-15%Al_2O_3, 100%Al_2O_3), 4 coating samples were prepared with different mixing ratios of alumina. The thickness of the coatings ranged between about 215 to 250μm. The detail of the spraying conditions is included in **Table 1**.

2.2 Microstructure characterization

The surface and cross section morphologies of the coatings were examined with an optical microscope and SEM to obtain the porosity and the content ratio of alumina splats in the coatings. Micro-structural characterization of coatings involves quantitative measurements of geometrical features such as porosity (in the form of voids, cracks and other defects) and analysis of material aspects of the coatings such as splat structure, interfaces, phases, etc[15]. In this research, the optical microscope is equipped with a CCD camera for image acquisition. Micrographs with two magnifications (200 X and 400 X) of the polished coating cross sections were used for

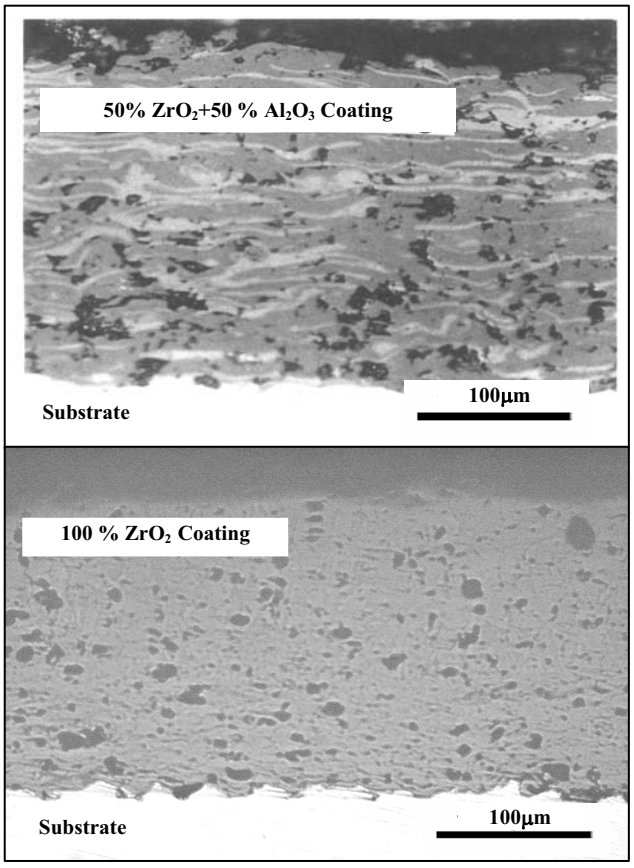

Fig.2 Cross-sectional SEM photos of composite coatings.

determining the porosity by image analysis software. It is clear that more pores are formed and that the lamella dimension is bigger in the coatings with lower alumina mixing ratio. The microstructure components can be represented in the images by gray level variation. Pores appear dark, which permit them to be distinguished and quantified. By rating the pore area to the cross-section, 2-D coating porosity assessments can be made.

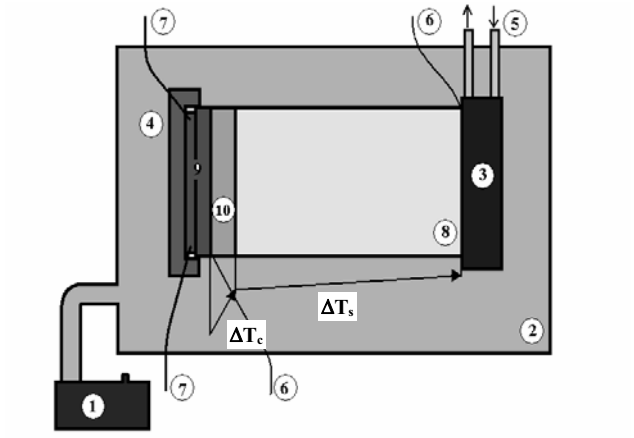

1.Vacuum pump; 2.Vacuum chamber; 3. Heat sink; 4. Heater holder, 5. Cooling water; 6. Thermal couples; 7. Heating power input; 8. Substrate; 9. Heater and heat buffer; 10. Coating

Fig.3 The parallel hot plates for thermal conductivity test.

On the other hand, all the samples were also examined with SEM on the coating cross-sections. **Figure 2** shows two typical SEM photos of the zirconia composite coatings. The SEM photos show clearly the coating microstructure characterized with pores and lamellae. In the SEM photos, the alumina lamellae appear brighter than zirconia content and the pores are the darkest. By comparing the alumina lamellae area to that of zirconia, the volume content ratio of alumina in the coatings can be assessed.

2.3 Parallel hot plates method

The thermal conductivity of the coatings can be calculated from the overall thermal conductivity of coating samples through the parallel hot plates method which measures the steady heat flux through the samples clamped in the two parallel hot plates. Nevertheless, the thermal conductivity of the stainless steel substrates should be firstly obtained using the pulsed laser heating method basing on the Laser Flash Thermal Constant Analyzer (Model:TC7000, ULVAC) and used to calibrate the results of the parallel hot plates method.

The laser flash technique can not be used to obtain the coating thermal conductivity because this method is based on the principle of measuring the transportation time through samples of the heat pulses produced by laser pulses. For homogeneous samples, the transportation time is easily related to the sample thickness and thermal diffusivity[16], while it is difficult to relate explicitly the transportation time to the sample thermal diffusivity for inhomogeneous samples.

The parallel hot plates method is shown schematically in **Fig. 3**. The assembly is mounted in a vacuum chamber in order to minimize the heat loss of the assembly surface to the ambient gas. The measured samples are prepared as about 25mmX10mmX3mm in dimension and are clamped between two parallel hot plates that are called the heater (higher temperature plate) and heat sink (lower temperature plate). Due to the high aspect ratio of the samples, the heat flux vertically through the coating and substrate is regarded as 1-D heat conduction while almost no error being introduced. Thus the coating region is in series with the substrate region when heat flux passing through them. The following expressions symbolize the heat conduction:

$$\begin{aligned} Q &= \eta_c S_c \frac{\Delta T_c}{d_c} = \eta_s S_s \frac{\Delta T_s}{d_s} = \eta S \frac{\Delta T}{d} \\ \Delta T &= \Delta T_c + \Delta T_s \\ d &= d_c + d_s \\ S &= S_c = S_s \end{aligned} \tag{1}$$

here S, ΔT, d and η are the sample surface area, temperature difference, sample thickness and sample thermal conductivity respectively and Q is the heat flux through the sample. The subscripts c and s are for the coating and the substrate region.

By solving the equation (1), the overall thermal conductivity of the samples can be expressed with some measured parameters of heat flux, Q, temperature difference crossing the sample, ΔT, the sample thickness, d and the sample surface area, S:

$$\eta = \frac{dQ}{\Delta T S} \tag{2}$$

The coating thermal conductivity can be then related to the overall thermal conductivity by the following equation that is an analogue to the expression for series circuit of electrical resistances:

$$\frac{d}{\eta S} = \frac{d_c}{\eta_c S_c} + \frac{d_s}{\eta_s S_s} \quad (3)$$

The equations (2) and (3) present the principle for coating thermal conductivity using parallel hot plates method. Letting the thermal resistance definition for any homogeneous layer carrying heat flux as the following:

$$R = \frac{d}{\eta S} \quad (4)$$

the equation (3) will take the form of $R=R_c+R_s$, which is the same as the formula for series circuit of electrical resistance.

According to equation (2), the heat flux, Q, passing through the samples clamped between the two parallel hot plates with a temperature difference of ΔT, is necessary for the overall sample thermal conductivity calculation procedure. In this research, the heat flux, Q, was directly replaced by the heating input power, P_{in}, into the higher temperature plate because the vacuum ambience reduced the ambient heat loss to a very low level and the heat flux through the samples to the heat sink is the only dissipation of the input power, i.e $Q=P_{in}$. The temperature difference, ΔT is measured by two thermal couples attaching to the both surfaces of the samples. In order to reduce the interface thermal resistance between the sample surfaces and the hot plate and to improve the thermal homogeneity between the thermal couples and sample surfaces, silicone grease was pasted into the interfaces. For each sample, four different heating powers were used and the thermal conductivity was measured four times to give an average, while the measurement precision was assessed.

Before the samples were measured, all the samples were polished on their surfaces using polishing papers up to No.1500, in order to improve the sample surface roughness and therefore the contact compactness between the samples and the hot plates.

3. Results and Discussions

3.1 Microstructure characterization results

From the SEM photos of the 4 different coating samples, two of them are shown in Fig.2, the coatings appear in porous and lamellar microstructures, the typical feature of this kind of plasma sprayed coatings. The SEM photos show the higher porosity in the samples with lower alumina mixing ratio, which is verified by the analysis results based on optical photos of the samples. The coating thickness of the samples was measured from their SEM photos. **Table 2** gives the thickness of the four different samples deposited with the same spraying time of 20μs but different alumina mixing ratio. The thickness variation arises simultaneously from the different deposition efficiency and the different stacking compactness of alumina splats from zirconia splats.

Table 2 Coating constituent and thickness.

Weight percentage (alumina)	100%	50%	20%	0%
Mole percentage	100%	41%	15%	0%
Volume percentage	100%	60%	27%	0%
Thickness	215μm	230 μm	245 μm	245 μm

Furthermore, the optical microscope photos were used to analyze quantitatively the porosity profile over the coating cross-sections and to get the average porosity. **Figure 4** shows the porosity and hardness profiles of the composite coating sample of $80\%ZrO_2+20\%Al_2O_3$ with a thickness of 245μm, which are both graded functional profiles over the coating cross-section. The average porosity of the composite coatings decreased almost linearly with the volume mixing ratio of alumina, as shown in **Fig.5**, and is due to the lower melting point and therefore higher molten degree of alumina powders than zirconia. Corresponding to the average porosity, the Vicker hardness of the coatings was also presented in Fig.5, which increased also linearly with the volume mixing ratio of alumina.

In conclusion, the addition of alumina into zirconia coatings lowered the coating porosity but increased the mechanical performance of hardness, both of which were good for the thermal barrier coating application of the composite coatings.

3.2 The calibration measurement

The measurements of the thermal conductivities of a bare stainless steel sample and a pure alumina coated stainless steel sample with the laser flash technique were used as the calibration for the parallel hot plates method and to get the thermal conductivity of stainless steel substrates for the calculation of the coating thermal conductivity following equation (3). The calibration procedure is necessary because the interface thermal resistance between the hot plates and the samples must be subtracted from the measured thermal resistance, when obtaining the coating thermal conductivity using equation (3). In fact, the laser flash technique measures

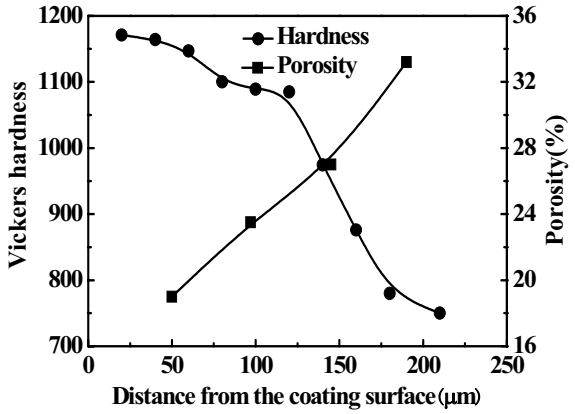

Fig.4 Hardness and porosity over the cross-section of composite coating.

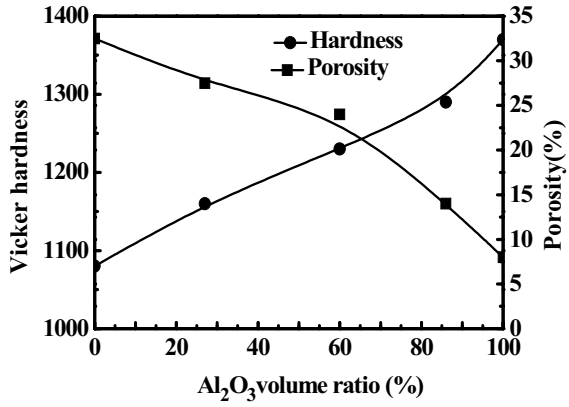

Fig.5 Effect of alumina volume ratio on average hardness and porosity of coatings.

the thermal diffusivity and thermal capacity instead of the thermal conductivity. For the stainless steel sample, the result is a thermal diffusivity of 414m^2/s and thermal capacity of 0.50J/g.K. From the density of stainless steel, 7.78g/cm^3, the thermal conductivity is calculated to be 16.08W/m.K, which is well consistent with the reference thermal conductivity of stainless steel of16.08W/m.K[17], For the pure alumina coated sample, the overall thermal diffusivity and average thermal capacity are 380m^2/s and 0.51J/g.K respectively. The average density of the coated sample is evaluated as 7.62g/cm^3 from the mass and volume of the sample. Accordingly the overall thermal conductivity of the sample is 14.77W/m.K and therefore the alumina coating should have a thermal conductivity of 4.42W/m.K (which is a little lower than the reference value of 5.80W/m.K because of the pores in the coating sample).

Then, a bare stainless steel sample and a pure alumina coated sample both with a dimension of 3mmX25mmX10mm were prepared for the calibration procedure of the parallel hot plate method. The measurements were performed also at 4 different heating powers. The average result of the bare sample was obtained as 13.8W/m.K, which is lower than that from the pulsed laser heat method. It is the difference of two results from which a calibration factor corresponding to the interface thermal resistance between the hot plates and the sample is obtained to be 0.124K/W. Based on the calibrated interface thermal resistance, the coating thermal conductivity of the pure alumina coating sample was calculated as 4.19 W/m.K from the overall thermal conductivity of 11.83W/m.K obtained by the hot plate method. Although the thermal conductivity of the pure alumina coating is lower than that from the pulsed laser method, the difference of only 5 percent demonstrated that the calibration for the parallel hot plate method should be credible for the other composite coating samples.

3.3 Effect of the microstructure on thermal conductivity

Figure 6 shows the upward tendency of the coating thermal conductivity with the alumina volume mixing ratio and **Fig. 7** gives the down-ward tendency of the thermal conductivity with the average porosity. The alumina additive increased the thermal conductivity of all the composite coatings, but all the sample coatings, even the pure alumina coating still have much lower thermal conductivities than bulk alumina. Nevertheless, the pure alumina coating has a thermal conductivity higher than that of bulk zirconia while the 2 real composite coatings have lower thermal conductivity than bulk zirconia. So, in conclusion, the zirconia composite coatings with alumina additive at weight mixing ratio up to 50% keep thermal resistance better than bulk zirconia, i.e, the addition of alumina up to 50% in weight did not reduce the coating thermal resistance.

The composite coatings are mixtures of three different components: alumina lamellae, zirconia lamellae and pores. Therefore the coating thermal conductivities are determined by both the basic thermal conductivities of the three components and the volume mixing ratio of the three components. According to the densities of the three components (in fact, only to the densities of zirconia and alumina: 6.0g/cm^3 and 4.0g/cm^3), the volume mixing ratio for each kind of the composite coatings can be calculated based on their weight mixing ratio. The result of volume mixing ratio is listed in **Table 2**. However, the splat stacking pattern in the composite coatings has also strong effect on the overall coating thermal conductivity, so the coating thermal conductivity can not be simply represented by the arithmetical average of the basic thermal conductivities of the three components weighted by their volume mixing ratios, which is as following:

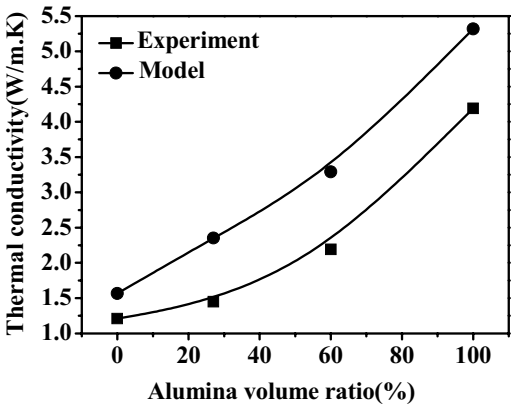

Fig.6 Dependence of coating thermal conductivity on alumina volume ratio.

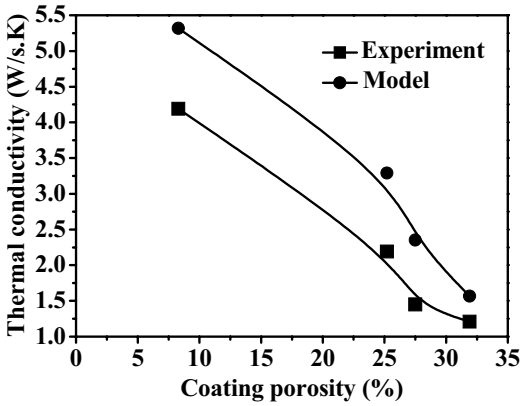

Fig.7 Dependence of coating thermal conductivity on coating porosity.

$$\eta_c^0 = (\eta_a \Gamma + \eta_z (1-\Gamma))(1-p) \quad (5)$$

Here, η_c^0, η_a, η_z, Γ and p are the arithmetical average of thermal conductivity, Al_2O_3 bulk thermal conductivity, ZrO_2 bulk thermal conductivity, alumina volume mixing ratio and porosity respectively.

In Fig 6 and 7, the theoretically arithmetical average thermal conductivities of the coatings were also presented. The theoretical thermal conductivity is always over-evaluated and but follows similar tendencies to the experiment tendencies both with volume mixing ratio of alumina and coating porosity. Although the composite coatings are mixed with three different components, each component of the coating is a stochastic stack of splats in stead of a homogeneous continuity and therefore the micro-interfaces between the splats have strong effects on the thermal conduction performance of coatings. In fact, many models[18] have been presented to simulate the thermal conduction behavior of mixed materials, but there is still no suitable model for sprayed composite thermal barrier coatings.

4. Conclusions

(1) The addition of alumina into zirconia thermal barrier coatings by gas tunnel type plasma spraying lowered the coating porosity and elevated the coating hardness, i.e, improved the microstructure and mechanical properties of the coatings from the view of thermal barrier application.

(2) Due to the lower porosity and higher thermal conductivity of alumina additive, the thermal conductivity of composite

coatings is increased in some extent. Nevertheless, the thermal conductivity of all the coating samples keeps lower than that of bulk alumina, while all the real composite coatings show lower thermal conductivity than bulk zirconia although the pure alumina coating shows higher thermal conductivity than bulk zirconia.

(3) The zirconia composite coatings with alumina additive at weight mixing ratio up to 50% keep thermal resistance better than bulk zirconia, i.e, the addition of alumina with weight mixing ratio up to 50% did not reduced the coating thermal resistance when compared with bulk zirconia.

Acknowledgement

This is supported financially by the Grant-in-aid of Japan Society for Science Promotion under NO.16.04371.

References

1) X.Q.Cao, R.Vassen and D.Stoever, Ceramic materials for thermal barrier coatings, Journal of Euro.Ceramic Society, 24(2004), pp.1.
2) V.Teixeira, M. Andritschky, W.Fischer, H.P. Buchkremer and D. Stover, Surf. Coat. Technol. 120-121(1999), pp103.
3) Y.Arata, A. Kobayashi,and Y.Habara, Ceramic coatings produced by means of a gas tunnel type plasma jet: J. Applied Physics, 62(1987), pp4884.
4) V.Teixeira, M.Andritschky, W.Fischer, H.P. Buchkremer and D.Stover, J. Mater. Process. Technol. 92-93 (1999), pp199.
5) R.Vassen, X.Cao, F.Tietz, D.Basu and D.Stover, Zirconates as new material for thermal barrier coatings. J. Am. Ceram. Soc., 83(8)(2000), pp2023.
6) J. Kaspar and O.Ambroz, Plasma coatings as thermal barriers based on zirconium oxide with yittrium oxide. In the first Plasma-technique-symposium, Vol.2, (Lucerne Switzerland, 18-20, May 1988), Ed. H.Eschnauer, P.Huber, A.R.Nicoll and S.Sandmeier. Plasma-Technique AG, Wohlen, Switzerland, pp.155-166 (1988).
7) R. Vassen and D. Stover, Functional gradient materials and surface layers prepared by fine particle technology, Kluwer Academiac Publishers, Netherlands, (2001), pp199.
8) G.Qian, T.Nakamura and C.C.Berndt, Mech. Mater. 27(1998), pp91
9) R.A.Miller, Thermal barrier coatings for aircraft engines: history and directions. J. Therm. Spray Technol., 6(1)(1997), pp35
10) H.Xie, H.Gu, Motoo Fujii and X.Zhang, Short hot wire technique for measuring thermal conductivity and thermal diffusivity of various materials, Meas. Sci. Technol., 17(2006), pp208
11) Silas E.Gustafsson, Transient hot strip method of measuring thermal conductivity and specific heat of solids and fluids, J. Appl. Phys., 53(9)(1982), pp6064.
12) J.J.Gonzalez, P.Proulx and M.Boulos, J. Appl. Phys., 74(1993), pp3065
13) Y.Arata, A.Kobayashi, Y.Habara and S.Jing, Gas tunnel type plasma spraying, Trans. of JWRI, 15-2(1986), pp.227.
14) A.Kobayashi, Formation of High hardness zirconia coatings by gas tunnel type plasma spraying, Surf .Coat. Technol., 90(1990), pp.197.
15) A.Kulkarni, Z.Wang, T.Nakamura and S.Sampath et al., Comprehensive microstructural characterization and predictive property modeling of plasma-sprayed zirconia coatings, *Acta. Mater.* 51(9) (2003), pp2457.
16) Y.Nagasaka and A.Nagashima, Simultaneous measurement of the thermal conductivity and thermal diffusivity, Rev. Sci. Instrum., 52(1983), pp229.
17) R.Vassen, G.Kerkhoff and D.Stover, Development of a mechanical life prediction model for plasma sprayed thermal barrier coatings, Mater. Sci. Eng., A303(2001), pp100.
18) I.H.Tavman, Effective thermal conductivity of granular porous materials, Int. Comm. Heat Mass Transfer, 23(1996), pp169.